ARCHAEOMETRIC STUDIES ON A BLUE GLASS FRAGMENT FROM POMPEII: CASE STUDY

Monica Gelzo[1], Gaetano Corso[1,2], Alessandro Vergara[3,4], Manuela Rossi[5], Oto Miedico[6], Ottavia Arcari[1], Antonio E. Chiaravalle[6], Ciro Piccioli[7], Paolo Arcari[1*]

[1]*Dipartmento di Medicina Molecolare e Biotecnologie Mediche, Università di Napoli Federico II, via S. Pansini 5, I-80131 Naples, Italy*
[2]*Dipartimento di Medicina Clinica e Sperimentale, Università di Foggia via L. Pinto 1, I-71100 Foggia, Italy*
[3]*Dipartmento di Scienze Chimiche, Università di Napoli Federico II via Cinzia 21, I-80126 Naples, 12 Italy*
[4]*Task Force di Ateneo sulle Metodologie Analitiche per la Salvaguardia dei Beni Culturali, Università di Napoli Federico II, Naples, Italy*
[5]*Dipartimento di Scienze della Terra, dell'Ambiente e delle Risorse, University of Napoles Federico II, Via Cinzia 21, I-80126 Naples, Italy*
[6]*Istituto Zooprofilattico Sperimentale di Puglia e Basilicata, via Manfredonia 20, I-71121, Foggia, Italy*
[7]*AIES Beni Culturali, I-80055 Portici, Naples, Italy*

GC and PA equally contributed to the work

ABSTRACT

A sample of Roman glass found in *Regio I, Insula 14,* during the 1950's Pompeii excavation was examined by Raman and Fourier transformed infrared spectroscopy, scanning electron microscopy, and inductively coupled plasma mass spectrometry. The analyzed specimen was selected based on its intense blue color and its well-preserved aspect. The purpose of the work was the chemical characterization of Pompeii's glass in correlation to the actual knowledge of Roman glassmaking technology from the Mediterranean area. The results suggested that the Pompeii's glass was a soda-lime-silica glass, but with a higher calcium content that, given the low content of lead, was used to stabilize the glass. The sample was in origin produced most likely as non-decolorized primary raw materials from eastern Mediterranean sites. Moreover, the intense blue color was related to the use mainly of cobalt, present in a weighty amount, and likely used as important coloring agents in the ancient secondary glass-making workshop.

1. INTRODUCTION

The production of Roman glass, as deduced from chemical analyses of specimens (dated from the first century B.C. up to the VII century A.D.) required two major components: sand and natron (probably Egyptian soda) mixed in appropriate proportions (Barfod et al., 2020). In particular, natron glass was made only in a few numbers of "primary" centers in Egypt and Syro-Palestine (Brill, 1988; Freestone, 2005; Jackson and Cottam, 2015). Several investigations were focused on the identification of the origin of the raw materials and the geographical location where the glass was produced (Wedepohl and Baumann, 2000; Freestone et al., 2003; Ganio et al., 2012; Petit-Domínguez et al., 2014). One major hypothesis suggested that glass production in primary workshops was performed in the Middle East (Huisman et al., 2009), in particular Palestine, using mainly the sand taken from the river Belus as a primary source. The sand was then mixed with natron, melted in furnaces, where dull black lumps were formed. Subsequently, the lumps broken into chunks were transported to workshops across the empire for shaping (Humphrey et al., 1998; Freestone, 2005; Degryse et al., 2014). Glasses fabricated only from silica and soda resulted unstable and subject to destruction from water. Therefore, glass stabilizers like lime (CaO) or lead (PbO) were required (Hodges, 1964), even though a low amount of these additives contributed to poor chemical durability of the glass while a higher amount rendered the glass prone to devitrification (Abd-Alla, 2007). The presence of alumina (Al_2O_3) or magnesia (MgO) prevented the devitrification of the glass (Hares GB, 1984).

Regarding Pompeii's glass manufacturers, many studies have been carried following Pompeii's excavations. Vallotto and Verità (2002), showed no great differences in the content of sodium oxide. In particular, the ratio between silicon and natron did not show great variability. Several Pompeian glasses showed similarity with the sand from the River Belus, thus suggesting the use by Pompeian workshops of primary glass row coming from the Middle East. Nevertheless, it cannot be excluded primary row glass production from other sites (perhaps the Volturno river or the provinces of Spain and Gaul) (Eichholz, 1962). Also, hundreds of Pompeian glass finds, classified as 'game counters', have been identified. These manufacturers were also described by Pliny the Elder (*Nat. Hist.* book XXXVI. Chap. 65) (Eichholz, 1962) as products of a melting recycling procedure leading to transparent, opaque, or widely colored objects, thus representing an example of glass production activities during the Roman epoch. Several studies on these finds were mainly finalized to the identification of

coloring or opacifying compounds (Mirti et al., 2002; Arletti et al., 2006; De Francesco et al., 2010; Cool, 2016). Moreover, Pompeii's excavations revealed the presence of glass production workshops probably dated before the Vesuvius eruption in 79 A.D. (De Francesco et al., 2010; Degryse et al., 2014).

Archaeometric methodology applied to cultural heritage is essential to obtain evidence on materials, production techniques, and habits of ancient people (Liritzis et al. 2020). In particular, the multidisciplinary approach allows solving archaeometry problems regarding glass production through Roman times. The present work aims to provide a further contribution to the knowledge of the materials and execution techniques used in Roman glass-making. Using different analytical approaches, we tried to determine the chemical composition of a Pompeian's blue glass fragment that, as an archaeological find, was quite rare and characterized by excellent durability and a good state of conservation. Moreover, we tried to highlight the technology used for its production.

2. MATERIALS AND METHODS

2.1. Light microscopy and X-ray diffractometry

The specimen was observed using a Nikon Eclipse L 150 reflected light microscope.

X-ray diffractometric analyzes (XRD) were carried out using a Miniflex Rigaku X-ray diffractometer with a Cobaltum tube, operating conditions 30 kV and 15 mA.

2.2. Scanning Electron Microscope

Textural and semi-quantitative chemical analyses were performed by using a scanning electron microscope (SEM) JEOL-JSM 5310, coupled with energy dispersive X-Ray spectroscopy (EDS). The setup operated at 15 kV primary beam voltage, 50–100 mA filament current, variable spot size, 20mm WD, and 40 s net acquisition in real-time. The apparatus was equipped with an Oxford Instruments Microanalysis unit and an INCA X-act detector using Energy software with an XPP matrix correction scheme and Pulse Pile-up correction. Data were processed with the INCA software, version 4.08 (Pouchou and Pichoir, 1991).

Back-scattered electrons (BSE) imaging and semi-quantitative chemical analyses were performed by pressing the glass to a flat surface and then coated with graphite. The sample has been placed at the same height as the cobalt standard used for routine calibration. Twenty analytical points were collected for each area and natural materials were used as standards. Energy dispersive spectroscopy (EDS) was used to evaluate the Co concentration.

2.3. Raman and FT-IR spectroscopy

Raman spectra were recorded using a confocal Raman microscope (NRS-3100, Jasco Applied Sciences, Halifax, Canada). The 514 nm line of an air-cooled Ar^+ laser (Melles-Griot) was injected into an integrated Olympus microscope and focused to a spot diameter of approximately 2 μm (100x or 20x objective), with a laser power of 4 mW at the sample. The spectral resolution was 6 cm^{-1}. Raman spectra were recorded at three separate spots on each paint powder to evaluate the heterogeneity. A holographic notch filter was used to reject the excitation laser line. Raman scattering was collected by a Peltier-cooled charge-coupled device photon detector (DU401BVI, Andor Technology, Belfast, Northern Ireland). A complete data set was collected in 100 s.

A small piece of glass (about 2.5 x 2 mm) was deposited on a 3-mm ZnS window and analyzed with a Nicolet 5700 equipped with a microscope Continuum (Thermo, West Palm Beach, FL. USA). Reflection spectra (200 acquisitions) were collected using the microscope focusing windows set at 50x50 μm. Spectra were analyzed by using the Omnic software. Peak assignment was further evaluated based on the data library (Socrates, 2001).

2.4. Inductively coupled plasma mass spectrometry

A fragment of the sample was grounded in a percussion apparatus used in geology. The sample resulted perfectly pulverized and preserved its blue color. The sample was then analyzed by Inductively coupled plasma mass spectrometry (ICP-MS).

In a first experiment (ICP-MS[a]), 100 mg of ground sample was subjected to mineralization in 2.5 ml of a mixture made of 1 part of HF (49% w/w) and three parts of HCl (37% w/w). Sample treatment was carried out inapposite containers in a microwave oven for 24 hours. The solubilized sample was then subjected to the ICP-MS analysis using Argon flux in an Agilent Technology 7506 apparatus (Santa Clara. California. USA).

A subsequent experiment (ICP-MS[b]) was carried out on about 50 mg of pulverized glass to detect trace elements (TE) and rare earth elements (REE). The total amount of the sample (46.8 mg) was split into two sub-aliquots (25.7 and 21.1 mg) and completely solubilized by using a reaction mix made of 6 ml HCl, 2 ml HNO_3 and 2 ml of HBF_4 (obtained by adding 30 g of boric acid to 100 ml of HF). Reaction vessels were placed into a microwave apparatus (Milestone Ethos-Easy supplied by FKV S.r.l. Italy). Acid digestion was carried out according to the following three steps: 1) temperature ramp from 25 to 220 °C for 20 min at 1600 watt. 2) 220 °C for 5 min at 1600 watt. 3) temperature ramp from 220 to 25 °C

for 40 min at 0 watts. The samples were then quantitatively recovered, brought to 50.0 mL with ultrapure water in disposable polypropylene falcon, and analyzed using the Nexion 2000 (PerkinElmer, Waltham, USA) inductively coupled plasma mass spectrometer (ICP-MS) equipped with a concentric nebulizer (Meinhard Associates, Golden, USA). A cyclonic spray chamber (Glass Expansion Inc., West Melbourne, Australia) and a quartz torch with a quartz injector tube (2 mm internal diameter) were used. To eliminate isobaric interferences, the kinetic energy discrimination (KED) system was used with helium (99.9999%. high purity) at 4.8 mL/min (high flow) for the determination of Fe. Cr. and V; at 3.7 mL/min (low flow) for the determination of Ni, Ca, As, Se, Co, Zn, Mn, and Cu. Standard mode (without any support gas) was employed for the determination of Li, Be, Mo, Ag, Sr, Sb, Sn, Ba, Cd, Hg, Tl, and Pb and for all the REE. A solution of Bi, Rh, Ga, and Re (approximately 100 ng/mL) was added online as internal standard by using a specific seven-lined mixing valve. To state, the concentration levels of each element were carried out as a preventive semi-quantitative analysis using a multi-element standard. Quantitative determination was carried out using the "internal additions" method in the mineralized solution (previously diluted 1:1 with ultrapure water to avoid the processing of a very acidic solution) through the use of calibration curves at four levels of spiking: for Li, Be, Ag, Cd, Tl, at 0.04 – 0.20 – 1.0 – 4.0 ng/ml; for V, Cr, Ni, Zn, As, Se, Mo, Sn, Sb, and Pb at 0.2 – 1.0 – 5.0 – 20 ng/mL; for Ba. Sr and Co at 1.0 – 5.0 –25 – 100 ng/mL; for Ca, Al, Mn, Fe, and Cu at 10 – 50 – 250 – 1000 ng/mL. For the 16 REE elements (in detail 14 REE with the addition of U and Th) was used the "internal additions" method at 4 – 20 – 100 – 400 pg/ml. Mg and Zr were determined only by a semi-quantitative method. The correlation coefficients (R^2) of standard calibration curves for all the trace elements were always higher than 0.999, showing a good linear relationship throughout the selected ranges of concentrations. Four mineralization blanks were carried out (the same reaction mix. without ceramic powder) and the mean concentration was subtracted for each element. The TE and REE concentrations were evaluated as the mean of both measurements. Good repeatability (less than 10%) was obtained for all the analytes, except for Cu, probably due to the uneven distribution of Cu salts in the ceramic matrix.

3. RESULTS AND DISCUSSION

3.1. Archaeological contest and glass sample characterization

The glass sample analyzed, a fragment of intense blue color (Fig. 1), was found in an amphora containing fragmented and intact glass manufactures in

Pompeii's excavation, *Reg. I, Insula 14, Casa 14* (Originally numbered as *Reg. II, Insula 14*, and successively, during 1950s excavations, changed to *Reg. I, Insula* 14). *Insula* 14 is located in the eastern area of the Regio I of Pompeii, in the median sector of the insulae gravitating on the eastern side via di Nocera and on the northern side via di Castricio that determines the prevailing orientation of the housing units. The first information about insula 14 dates back to 1954, the period in which Amedeo Maiuri began an important excavation season to bring to light the entire southeastern sector of the city. In the first phase, the investigations were limited to freeing the southern front between insulae 13 and 14, and only in 1957, the southeast corner was reached, identifying a thermopoly pertaining to the current number 15. After the excavation and consolidation of the wall hills that emerged, the research activity was interrupted and resumed in 1984 (D'Anna, 2020). The archaeological period of the glass finds was attributable to the earthquake described by Tacitus and Seneca that seriously damaged Pompeii in AD 62. However, according to some views, the AD 62 earthquake (defined as *terminus post quem*) was not a single event but other seismic activity, occurred over a certain number of years (Neronian and early Flavian periods) (Keenan-Jones, 2015), generated stratigraphic sequence due to the subsequent demolition and rebuilding thus, suggesting that not all the glass finds have been precisely contemporaneous. All excavated specimens should have been preserved from subsequent potential deterioration caused by the eruption of Vesuvius in 79 AD (*terminus ante quem*) (Cool, 2016). Dr. Piccioli, C., an official of the former Archaeological Superintendence of Naples and Caserta (SANC) selected the distinctive sample that was considered, according to archaeological caution, well preserved and of great significance, because its intense color that appeared identical to that of other intact glass manufactures. The artifact (about 2x3 cm) was carefully handled to avoid additional contamination and softly cleaned with a brush and wet bibula paper to remove dust deposits. The fragment was then stored in a preserved area to avoid further environmental deterioration. The sample did not show any opacity. The glass color, according to the Munsell notation, was organoleptically corresponding to a saturated and intense color (Cochrane, 2014). Reflected light microscopy observation revealed some technical properties such as the absence of bubbles and the refinement in cooking which explained the durability of the material. The glass surface appeared non-homogeneous highlighting forms of yellow, white, and dark blue pitting alterations most likely attributable to the chromophoric elements responsible for the blue color whereas, no crystalline phases were observed by X-ray diffraction (XRD) from three independent diffractogram peaks representing the intensity of a certain reflection in a certain glass orientation (not shown). These findings suggested the absence of devitrification and excellent quality of the glass also in consideration of the elapsed time. Under this aspect, it must be pointed out that degradation or deterioration of buried archaeological glass can be caused by both external factors, like environmental conditions, and/or internal factors, such as glass chemical composition, that might lead to a partial or complete loss of its properties. In particular, glasses rich in natrum might present the lowest grade of corrosion (associated with the formation of a silica-rich protective film often depleted in alkalis) whereas, glasses rich in potassium or lead highlight deeper corrosion (associated with the formation of an external non-protective Al_2O_3-SiO_2 layer, or with a thicker external layer of corrosion and a significant depletion of K_2O) (Zacharias et al., 2020). Therefore, it might be possible that the conservation conditions that occurred after the eruption of Vesuvius preserved the buried glasses from a strong degradation process.
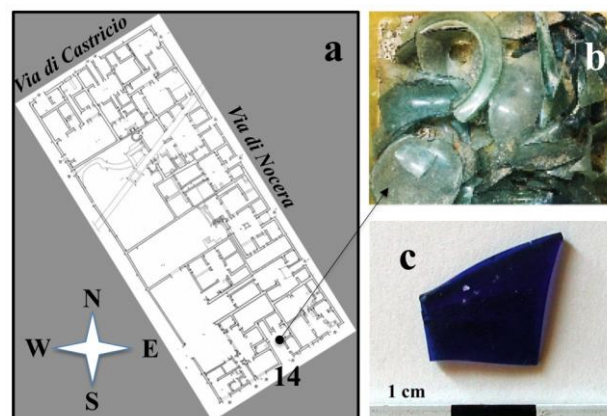

Figure 1. (a) *Recent planimetry of the Regio I, Insula 14, Casa 14 (archive of Archaeological Park of Pompeii) where the amphora containing intact and glass fragments **(b)** were found. **(c)** Blue glass sample analyzed*

3.2. Raman and FT-IR spectroscopy

Raman spectrum of the sample, reported in Fig. 2a, highlighted the presence of two major peaks at 1090 and 584 cm^{-1} with and two well-defined components at 945 and 995 cm^{-1}. This signature corresponded to common lime-based glass (typically having a composition with about 10 to 15% Na_2O, and about 8 to 15% CaO). In some cases, only one shoulder was observed at 950 or 995 cm^{-1} (Koleini et al., 2019). The two major signatures are associated with the Si-O bending (~550 cm^{-1}) components of SiO_4 entities of the more or less polymerized (Si-O)n framework, and Si-O stretching (~1090 cm^{-1}) (Caggiani et al., 2014). The feature at 773 cm^{-1} is usually assigned to the vQ_0 mode of isolated not-bridged SiO_4 entities (Colomban et al., 2006). The maximum of the SiO_4 bending and stretching bands in the general database was determined from the Raman characterization of hundreds of different types of glassy silicate whose elemental compositions were determined by classical methods, thus allowing the identification of different types of glass (Colomban et al., 2021). Studies made by Colomban et al., 2006, highlighted families of glasses based on the relationship between the Raman peak area ratio (A500/A1000), defined as polymerization index I_P, of envelopes and wavenumbers of the different Si-O stretching components. The empirical relationship between I_P, glass composition, and the processing temperature was rather well documented (Colomban and Paulsen, 2005). According to this classification, the I_p value calculated from Raman spectra collected in a different area of the sample ($I_p = 0.6 \pm 0.05$) would correspond to a family of silicate-based glasses characterized by an intermediate ratio between flux components ($Na_2O + K_2O + CaO$) with a very low content of PbO and most likely processed at medium temperature. Regarding the blue color and opacifiers, Raman features did not suggest either the detectable amount of lazurite $(Na,Ca)_8(SO_4,S,Cl)_2(AlSiO_4)_6$ (Caggiani et al., 2014) or $Ca_2Sb_2O_7$ (no 672 cm^{-1} bands) (Neri et al., 2016).

The Fourier transformed infrared (FT-IR) spectra of the sample (Fig. 2b) showed a profile with the presence of bands consistent with the Raman result. Typical spectra showed broadband in the 3590 cm^{-1} regions arising from stretching of the –OH most likely assigned to the silanol group or in adsorbed water in the sample. The spectrum was characterized by bands at 2926–2844 cm^{-1} (functional groups region) and 1725–1586 cm^{-1} (double bond stretching) regions because of C-H bending (Derric, 1989; Gelzo et al., 2014), which could be due to some original organic contamination of organic structures on the silica's surface. Peaks at 1264, 893, and 798 cm^{-1} could be assigned to Si-O symmetrical stretching vibration, Si-OH bending, and SiO_2 stretching, respectively (Torres-Carrasco et al., 2014; Gentelli and Medhat, 2017).
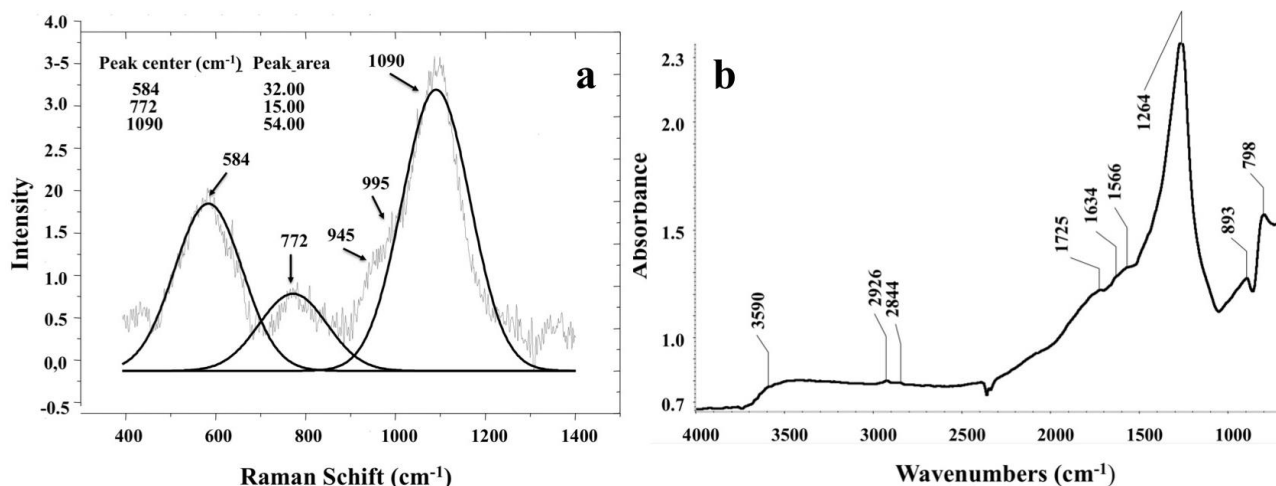
Figure 2. Raman spectra (a) and representative FT-IR spectra (b) of Pompeian's blue glass

3.3. Scanning Electron Microscope

Back-scattered electrons (BSE) in scanning electron microscope (SEM) imaging showed non-homogeneity of the sample (Fig 3A). The semi-quantitative analysis was characterized by a great variability (high S.D. and CV%) because observations were made on different areas of the glass surface. Areas of the sample showed the presence of CoO up to a concentration of about 2.0 wt% and 6.0 wt%, Fig. 3B and 3C (light gray zones), respectively whereas, in other areas, the CoO content ranged from zero to about 1.0 wt%. PbO ranged from zero to about 6.0 wt%. Ti and Fe were also detected as well as minerals attributable to the group of zeolites likely formed by the alteration of glass (Frugier et al., 2017). Table 1 shows the average composition of the glass. The sample appeared as a soda-lime-silica glass with the average concentration

of SiO₂, Na₂O, and CaO of 61.71 wt%, 1.44 wt%, and 5.16 wt% respectively, although the average Na₂O concentration resulted lower compared to that reported in the literature data on glasses of the period (De Francesco et al., 2019) whereas, a higher average concentration of MnO, FeO, CoO, and PbO was observed. The latter data suggested that cobalt was most likely the key chromophoric element responsible for the sample blue color (Verità, 2004; Silvestri et al., 2005; Panagopoulou et al., 2018).
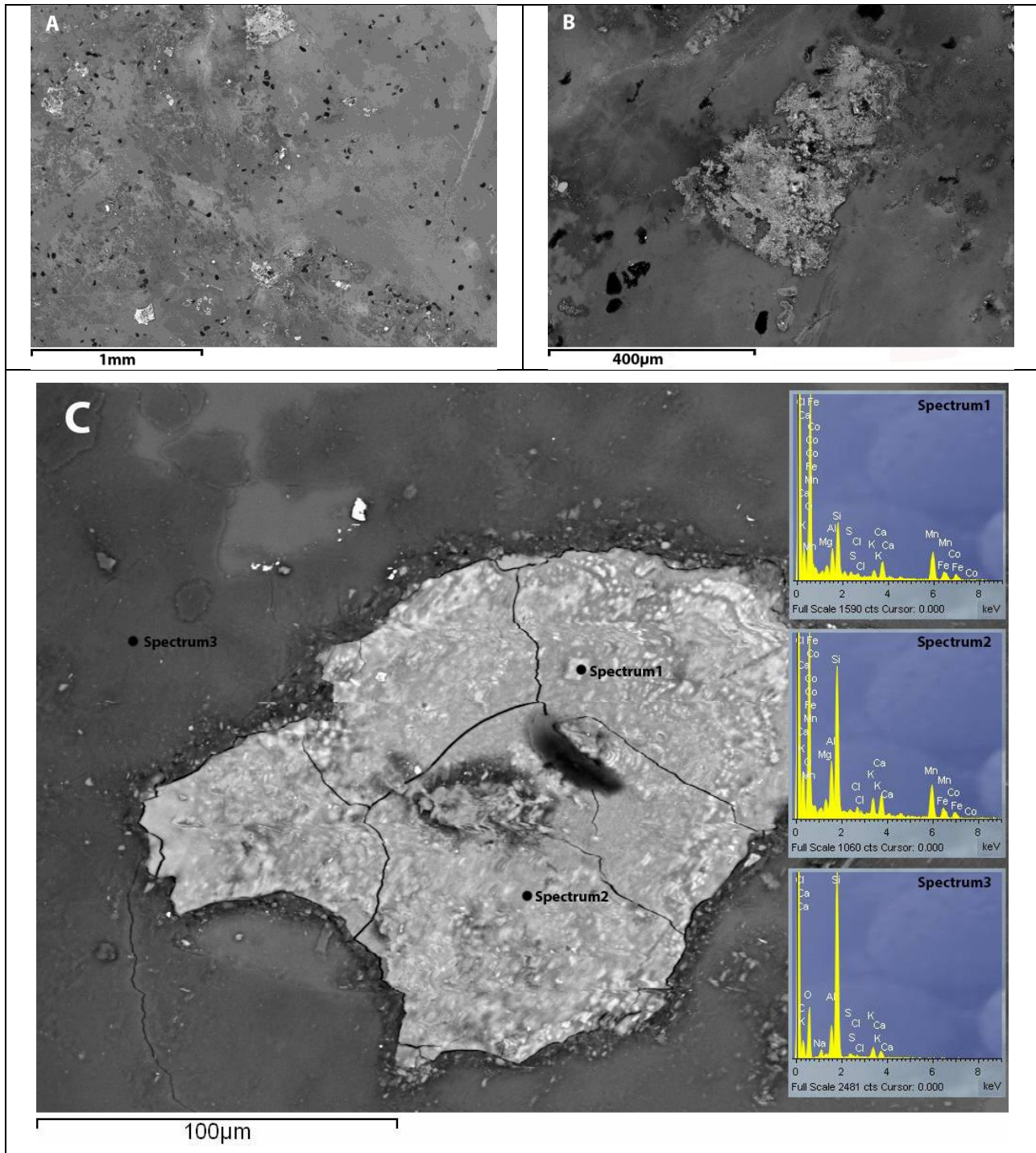

Figure 3. BSE images of the Pompeii's blue glass. A. Image showing the variable composition of the sample. B. Sample area containing about 2 w% of Co (area with a light gray). C. Sample area containing about 6 w% of Co (area with light grey) and the EDS corresponding spectra (insets) recorded in a different spot for the sample of the evaluation of Co concentration.

Oxides	Average w%	SD	CV %
SiO_2	61.71	16.41	26.59
Na_2O	1.44	1.71	118.75
MgO	1.71	3.01	176.02
P_2O_5	0.62	2.10	338.71
SO_3	1.07	0.63	58.88
CaO	5.16	6.85	132.75
TiO_2	0.61	0.61	100.00
MnO	5.54	6.18	111.55
FeO	3.37	3.30	97.92
CoO	1.16	1.53	131.90
PbO	1.24	1.85	149.19
F	1.25	3.28	262.40
Cl	1.89	5.76	304.76

SD, Standard Deviation; CV, Coefficient of Variability

3.4. Inductively coupled plasma mass spectrometry

Because inductively coupled plasma mass spectrometry (ICP-MS) measurements of silicon at m/z 28 suffer from numerous spectral interferences that could include C, O, and N (the latter most likely coming from nitric acid), we first analyzed the presence of trace elements (TE) in the Pompeian glass powder after its digestion in HF and HCl in a 1:3 ratio (ICP-MS[a]). We expected a Si concentration above detection limits thus, it was not necessary to pre-concentrating the sample. Silicon does not require significant amounts of strong acid and low levels (< ~10 ppm) are soluble and stable in water. Moreover, the ICP-MS used allowed Si measurements in the range of a few ppm. The ICP mass analytical results are summarized in Table 2. In particular, the sample showed a relatively high content of Si, Na, and Ca and a lower content of Fe, Al, Co, Mn, Cu, Sb, Pb, and K. The amount of these elements, converted in the corresponding oxides, highlighted a composition similar to that observed in several Roman glasses (De Francesco et al., 2010). In fact, the percentage (w%) of SiO_2, Na_2O, CaO, Al_2O_3, K_2O, MgO, FeO, MnO, PbO, and CuO were 43.8, 5.6, 5.4, 1.0, 0.66, 0.28, 0.7, 0.24, 0.09, and 0.08, respectively. The MgO and K_2O compositions were less than 1.5%. This data suggested that natron was the primary alkali flux for this glass (Liritzis et al., 1995, Henderson, 2013; Alawneh et al., 2017). It is also worth noting that the amount of Sb observed (0.99 w%) was not sufficient as an antimony-based opacifier as instead observed for other Roman and Pompeian glasses (Kaplan et al., 2017; De Francesco et al., 2019).

ICP-MS was used was also performed after-treatment of the sample with HCl, HNO_3, and HBF_4 at a 2:1:1 ratio (v/v) in a temperature ramp (ICP-MS[b]). The results are reported in Table 2. Although with this procedure it was not possible to detect Si, K, and Na, also here was observed a moderate-high content of Fe, Al, Ca, Co, Mn, Cu, and Mg. The weight percentage (w%) of the corresponding oxides FeO, Al_2O_3, CaO, CoO, MnO, CuO, and MgO were 0.79, 2.74, 8.06, 0.20, 0.52, 0.68, and 0.65, respectively (Scott and Degryse, 2014). The CaO content evaluated by ICP-MS[a] and ICP-MS[b] (5.4 w% and 8.05 w%, respectively) was slightly higher compared to that reported for Pompeian glasses by De Francesco et al., 2019 (average 7.215%) and according to the literature data on a glass of the period (Verità, 2004; Silvestri et al., 2005; Arletti et al., 2006; Degryse and Schneider, 2008; Foster and Jackson, 2009; Fermo et al., 2016). This value could be related to the percentage of sodium present in the natron to flux the silica (Jackson and Cottam, 2015; Cottam and Jackson, 2018) and the higher quantity of lime was used to stabilize the glass thus, suggesting that the sample represented a specialized production, perhaps using a plant-ash component, during the 1st century A.D.

The relationship between the composition of Al_2O_3 (1.0 w% by ICP-MSa and 2.74 w% by ICP-MSb) and that of CaO showed to be very close to that reported for Pompeii glasses within the area of Roman Western European sites and in the Mediterranean area in the 1st - 3rd century A.D. (Gallo et al., 2013). As suggested, these values could be due to the employment for the glass productions of similar raw materials along with the Empire and most likely from the Middle-East region (Silvestri et al., 2005; Al-Bashaireh et al., 2016; Nenna et al., 1997; Picon and Vichy, 2003; Silvestri, 2008; Liritzis et al., 2018).

The relatively high content of FeO (0.7 w% by ICP-MS[a] and 0.79 wt% by ICP-MS[b]) as already reported by De Francesco et al., (2019) can be found in blue-colored Roman glasses. However, its amount might be depending upon the MnO concentration. In this case, the manganese oxide concentration (0.24 w% by ICP-MS[a] and 0.52 wt% by ICP-MS[b]) was within natural limits, thus suggesting the use of iron-containing raw material that was most likely not subjected to the decoloring procedure. Decolorized glasses generally show MnO concentration > of 0.5 wt% probably due to the addition of manganese as pyrolusite (MnO_2) (Jackson, 2005). The latter was particularly widespread in the Roman period to neutralize the color due to the iron oxides naturally present in the primary raw materials (Silvestri et al., 2005 Jackson, 2005; Silvestri, 2008, Gliozzo, 2017). These findings support the hypothesis that the Pompeian glass could have been produced from the sands from the Middle-East region (Foy et al., 2003).

Also, copper and cobalt, contained in the sample at a concentration of 5467 ppm and 1615 ppm, respec-

tively (0.20 w% and 0.68 w% by ICP-MS) were important coloring agents in the ancient glass-making workshop (Mirti et al., 2002; Hodgkinson and Frick, 2020). For instance, copper might produce blue color depending on its interaction with iron and on some level with manganese and lead. However, deep blue glass showed significant amounts of copper and cobalt in the order of 1930 ppm and 1453 ppm (Arletti et al., 2008), Therefore, the deep blue color of the sample, besides the iron present in the raw material, might be due to the presence of copper and cobalt probably added as $2Co_2O \cdot CuO \cdot 6H_2O$ (trianite). This compound was often used for the production of Roman blue glass (Arletti et al., 2008). Therefore, as also clearly shown by BSE imaging (Fig. 3B and 3C), the blue color of the glass sample was essentially due to cobalt probably used in Pompeian secondary furnaces for glasses manufacture production (De Francesco et al., 2019).

ICP-MS[b] was also used to determine the content of rare earth elements (REE). The results, reported in Table 2, showed that neodymium (Nd) was the most preponderant rare earth element present in the sample with a concentration of 13.629 ppm. This element belongs to the light rare earth elements (LREE) of the lanthanide series and its concentration is in the range of the concentration of Nd in silica-based, non-carbonaceous sediments and sedimentary rocks that generally is in the order of 5–50 ppm (Faure and Mensing, 2005x). Neodymium content in glass components such as shell and limestone as well as natron is much lower (around 0.5-10 ppm, and 20-40 ppb, respectively (Faure and Mensing, 2005; Wedepohl 1978; Wedepohl et al., 2011). These findings suggest that Roman glasses were originated from heavy minerals or a fraction of non-quartz minerals of the silica-based raw material (Degryse and Schneider, 2008). Under this aspect, sands from the Campanian beaches by the Garigliano and Volturno Rivers were likely not used in this case (Brems et al., 2012) since this area all contained more Nd, even up to 296 ppm (Brems et al., 2013). Moreover, these sands contained high percentages of heavy minerals, resulting in high Fe_2O_3 and Al_2O_3 levels, making them unsuitable for glass production (Degryse and Schneid, 2008; Brems et al., 2009).

Table 2. Elemental composition of Pompeii's blue glass sample evaluated by ICP-MS

TE	Average μ/g (ppm)	SD (CV 17%)	Average mg/100mg	Average μ/g (ppm)	SD (CV 15%)	Average mg/100mg	REE	Average μ/g (ppm)	S.D. (CV 15%)
		ICP-MS[a]				**ICP-MS[b]**			
V	n.d.	-	n.d.	11.98	1.80	0.0012	Y	7.595	1139.2
Cr	30.0	5.1	0.003	14.43	2.16	0.0014	La	9.725	1458.7
Fe	2550.0	433.5	0.255	6166.24	924.94	0.6166	Pr	1.715	257.3
Al	3160.0	537.2	0.316	14510.16	2176.52	1.4510	Nd	13.629	2044.4
Ni	110.0	18.7	0.011	67.33	10.10	0.0067	Sm	1.466	220.0
Ca	39100.0	6647	3.91	57580.72	8637.11	5.7581	Eu	0.435	65.3
As	10.0	1.7	0.001	18.31	2.75	0.0018	Gd	1.588	238.3
Se	n.d.	-	n.d.	1.82	0.27	0.0002	Tb	0.220	22.1
Co	340.0	57.8	0.034	1615.30	242.29	0.1615	Dy	1.277	191.7
Zn	n.d.	-	n.d.	53.62	8.04	0.0054	Ho	0.249	37.5
Mn	1100.0	187	0.110	4084.11	612.62	0.4084	Er	0.752	112,8
Cu	660.0	112.2	0.066	5467.89	820.18	0.5468	Tm	0.099	15.0
Li	n.d.	-	n.d.	<1	-	< 10^{-5}	Yb	0.642	96.3
Be	n.d.	-	n.d.	<1	-	< 10^{-5}	Lu	95.07	14.3
Mo	n.d.	-	n.d.	5.33	0.80	0.0005	Th	0.865	129-9
Ag	n.d.	-	n.d.	<1	-	< 10^{-5}	U	0.924	138.7
Sr	320.0	54.4	0.032	504.72	75.71	0.0505			
Sb	9940.0	1689.8	0.994	23.33	3.50	0.0023			
Sn	n.d.	-	n.d.	<3	-	< 10^{-5}			
Ba	1500.0	255	0.150	261.12	39.17	0.0261			
Cd	n.d.	-	n.d.	<0.5	-	< 10^{-5}			
Hg	n.d.	-	n.d.	<0.1	-	< 10^{-5}			
Tl	n.d.	-	n.d.	0.054	0.008	0.0000			
Pb	870.0	147.9	0.087	10.89	1.63	0.0011			
Mg	1740.0	295.8	0.174	3960.45	594.07	0.3960			
Zr	n.d.	-	n.d.	35.11	5.30	0.0035			
K	2740.0	465.8	0.274	n.d.	-	n.d.			
Si	205000.0	34850	20.5	n.d.	-	n.d.			
Na	42000.0	7140	4.20	n.d.	-	n.d.			
Ti	220.0	37.4	0.022	n.d.	-	n.d.			

TE, Trace Elements; REE, Rare Earth Elements; SD, Standard Deviation; CV, Coefficient of Variability

4. CONCLUSIONS

In this study, by applying a combination of Raman and FTIR spectroscopy, SEM, and ICP-MS, the chemical composition of a Pompeian's glass blue fragment has been determined, thus representing a possible contribution to the archaeological knowledge on Pompeian's glass manufactory. The sample appeared as a refined glass and was most likely obtained from secondary raw materials. By evaluating the composition of the sample, we tried to define possible areas where suitable sand raw materials would have been available.

The glass sample analyzed was a soda-lime-silica glass containing a slightly higher CaO content most likely used to stabilize the glass. Moreover, as suggested by the Ip value, the sample was a lower lead-based silicate most likely processed at medium temperature. Furthermore, the amount of Al_2O_3 and CaO suggested the employment of similar raw materials along with the Empire and most likely that from the Middle-East region. The Nd content (ppm) of the blue sample, excluded the use of the sand of Campanian beaches for primary raw material.

The FeO content was within natural limits and closer for other Roman glasses thus indicating the use of iron-containing raw material that was not subjected to the decoloring procedure.

The deep blue color was most likely due to the cobalt, present in a substantial amount, and possibly used as an important coloring agent in the secondary glass-making workshop.

These results suggested the presence of the primary glass production industry and a possible Pompeian secondary workshop for the production of glass manufactures during the first century AD.

AUTHORS' CONTRIBUTION

MG, OM, and AEC were involved in ICP-MS sample analyses. CP and OA were involved in the archaeological classification of the sample. AV performed Raman spectroscopy and analysis of the data. MR was involved in SEM analysis and data interpretation. GC and PA made contributions to the interpretation of data, drafting, and revision of the manuscript. All authors have read and approved the final manuscript.

REFERENCES

Abd-Alla, R. 2007. devitrification behavior of corroded glass: four cases study. *Mediterranean Archaeology and Archaeometry*. Vol. 7, pp. 39-49.

Al-Bashaireh, K., Alama, E., Al-Housan, A.Q. 2016. Analytical and Technological Study of Roman, Byzantine and Early Islamic (Umayyad) Glasses from Al-Fudein Archaeological Site, Jordan. *Mediterranean Archaeology and Archaeometry*. Vol. 16, pp. 257-268.

Alawneh, F., Al Shiyab, A., Al Sekheneh, W. 2017. Chemical analysis of late roman glass from Qasr al Rabbah, Jordan. *Mediterranean Archaeology and Archaeometry*. Vol. 17, pp. 201-213.

Arletti, R., Dalconi, M. C., Quartieri, S., Triscari, M., Vezzalini, G. 2006. Roman Coloured and opaque glass: a chemical and spectroscopic study. *Applied Physics A*. Vol. 83, pp. 239-245.

Arletti, R., Vezzalini, G., Biaggio Simona, S., Maselli Scotti, F. 2008. Archeometrical studies of Roman Imperial Age glass from Canton Ticino. *Archeometry*. Vol. 50, pp. 606-626.

Arletti. R., Ciarallo, A., Quartieri, S., Sabatino, G., Vezzalini, G. 2006. Archaeometric analyses of game counters from Pompeii. In: M. Maggetti, B. Messiga, (Eds). *Geomaterials in Cultural Heritage*. Geological Society, London, Special Publications, 257, pp. 175–186.

Barfod, G.H., Ian C. Freestone, I.C., Lesher, C.E., Lichtenberger, A., Raja, R. 2020 'Alexandrian' glass confirmed by hafnium isotopes. *Scientific Reports*. Vol. 10, 11322.

Brems, D., Boyen, S., Ganio, M., Degryse, P., Walton, M. 2009. Mediterranean sand deposits as a raw material for glass production in Antiquity. In: Ignatiadou, D., Antonaras, A. (Eds). *Annales du 18e Congrès de l'Association Internationale pour l'Histoire du Verre Thessaloniki*. pp. 120-127.

Brems, D., Degryse, P., Hasendoncks, F., Gimeno, D., Alberta Silvestri, A., Vassilieva, E., Luypaers, S., Honings, J., 2012. Western Mediterranean sand deposits as a raw material for Roman glass. Production. *Journal of Archaeological Science*. Vol. 39, e2907.

Brems, D., Ganio, M., Latruwe, K., Balcaen, L., Carremans, M., Gimeno, D., Silvestri, A., Vanhaecke, F., Muchez, P., Degryse, P. 2013. Isotopes On The Beach, Part 2: Neodymium Isotopic Analysis for the Provenancing of Roman Glass-Making. *Archaeometry*. Vol. 55, pp. 449–464.

Brill, R.H. 1988. Scientific investigations of the Jalame glass and related finds. In: Gladys Davidson Weinberg, G.D. (Ed.), *Excavations at Jalame. Site of a glass factory in late Roman Palestine*. Missouri Press, Columbia, pp. 257-294.

Caggiani, M.C., Acquafredda, P., Colomban, P., Mangone, A. 2014. The source of blue color of archaeological glass and glazes: the Raman spectroscopy/SEM-EDS answers. *Journal of Raman Spectroscopy*. Vol. 45, pp. 1251–1259.

Caggiani, M.C., Valotteau, C., Colomban, P. 2014. Inside the glassmaker technology: search of Raman criteria to discriminate between Emile Gallé and Philippe-Joseph Brocard enamels and pigment signatures. *Journal of Raman Spectroscopy*. Vol. 45, pp. 456-464.

Cochrane, S. 2014. The Munsell Color System: A scientific compromise from the world of art. *Studies in History and Philosophy of Science Part A*. Vol. 47, pp. 26-41.

Colomban, P., Aurélie Tournie, A., Bellot-Gurlet, L. 2006. Raman identification of glassy silicates used in ceramics, glass and jewellery: a tentative differentiation guide. *Journal of Raman Spectroscopy*. Vol. 37, pp. 841-852.

Colomban, P., Franci, G.S., Farahnaz Koleini, F. 2021. On-Site Raman Spectroscopic Study of Beads from the Necropolis of Vohemar, Northern Madagascar (>13th C.). *Heritage*. Vol. 4, pp. 524–540.

Colomban, P., Paulsen, O. 2005. Non-Destructive Determination of the Structure and Composition of Glazes by Raman Spectroscopy. *Journal American Ceramic Society*. Vol. 88, pp. 390-395.

Cool, H.E.M. 2016. Recreation or decoration: what were the glass counters from Pompeii used for? *Papers of the British School at Rome*. Vol. 84, pp. 157–177.

Cottam, S., Jackson, C.M. 2018. Things that traveled: Precious things for special people? In: D. Rosenow, M.Phelps, A. Meek, I. Freestone (Eds.). *Mediterranean Glass in the First Millennium CE*. UCL Press University College, London, pp. 92-106.

D'Anna C. 2020. Pompei, Regio I insula 14. I rivestimenti pavimentali del civico 15. In Atti del XXVI *Colloquio dell'Associazione Italiana per lo Studio e la Conservazione del Mosaico*, Roma 18-21 marzo pp. 413-426.

De Francesco A.M., Scarpelli R.1, Conte M., Toniolo L. 2019. Characterization of Roman glass from Casa Bacco deposit at Pompeii by wavelength-dispersive electron probe microanalysis (EPMA). *Mediterranean Archaeology and Archaeometry*. Vol. 19, pp. 79-91.

De Francesco, A.M., Scarpelli, R., Barca, D., Ciarallo, A., Buffone, L. 2010. Preliminary chemical characterization of Roman glass from Pompeii. *Periodico di Mineralogia*. Vol. 79, pp. 11-19.

Degryse, P., B. Scott. R.B., Brems, D. 2014. The archaeometry of ancient glassmaking: reconstructing ancient technology and the trade of raw materials. *Perspective*. Vol. 2, pp. 224-238.

Degryse, P., Schneider, J. 2008. Pliny the Elder and Sr–Nd isotopes: tracing the provenance of raw materials for Roman glass production, *Journal of Archaeological Science*. Vol. 35, pp. 1993–2000.

Derrick, M. 1989, Fourier transform infrared spectral analysis of natural resins used in furniture finishes. *Journal of the American Institute for Conservation*. Vol. 28, pp. 43–56.

Eichholz, D.E. 1962. Volume X: Pliny. Natural History Books 36-37. Cambridge, MA. Harvard Loeb Classical Library 419. Cambridge, MA: Harvard University Press.

Faure, G., Mensing, T. M. 2005. Isotopes: principles and applications, 3rd edn, Wiley, New York.

Fermo, P., Andreoli, M., Bonizzoni, L., Fantauzzi, G., Giubertoni, G., Ludwing, N., Rossi, A. 2016. Characterisation of Roman and Byzantine glasses from surroundings of Thugga (Tunisia): Raw material and colours. *Microchemical Journal*. Vol. 129, pp. 5-15.

Foster, H.E., Jackson, C.M. 2009. The composition of naturally coloured late Roman vessel glass from Britain and the implications for models of glass production and supply. *Journal of Archaeological Science*. Vol. 36, pp. 189– 204.

Foy, D., Picon, M., Vichy, M., Thirion-Merle, V. 2003 Caractérisation des verres de la fin de l'Antiquité en Méditerranée occidentale: l'émergence de nouveaux courants commerciaux. In: Foy, D. and Nenna,

M.D. (Eds.), *Échanges et commerce du verre dans le monde antique. Actes du colloque de l'Association Française pour l'Archéologie du Verre*, Aix-en-Provence et Marseille, 7-9 juin 2001. Editions Monique Mergoil, Montagnac, pp. 41-85.

Freestone, I.C. 2005. The Provenance of ancient glass through compositional analysis. *Materials Research Society Symposium Proceedings. Vol.* 852, pp. 8.1.1-8.1.14.

Freestone, I.C., Leslie, K.A., Thirlwall, M., Gorin-Rosen, Y. 2003. Strontium isotopes in the investigation of early glass production: Byzantine and early Islamic glass from the near East. *Archaeometry. Vol.* 45, pp. 19-32.

Frugier, P., Fourniera, M., Gina, S. 2017. Modeling resumption of glass alteration due to zeolites precipitation. *Procedia Earth and Planetary Science*. Vol. 17, pp. 340 – 343.

Gallo, F., Silvestri, A., Molin, G. 2013. Glass from the Archeological Museum of Adria (North-East Italy): new insights into Early Roman production technologies. *Journal of Archaeological Science*. Vol. 40, pp. 2589-2605.

Ganio, M., Boyen, S., Fenn, T., Scott, R., Vanhoutte, S., Gimenoc, D. 2012. Roman glass across the Empire: an elemental and isotopic characterization. Journal of Analytical Atomic Spectrometry. Vol. 27, 743.

Gelzo, M., Grimaldi, M., Vergara, A., Severino, V., Chambery, A., Dello Russo, A., Piccioli, C., Corso, G., and Arcari, P. 2014. Comparison of binder compositions in Pompeian wall painting styles from Insula Occidentalis. *Chemistry Central Journal*. Vol. 8, 65.

Gentelli, L., Medhat, A. 2017. A multi-analytical approach for the archaeometry identification of a Roman period glass furnace in the central Nile delta. *Journal of Archaeological Science: Reports*. Vol. 11, pp. 330–337.

Gliozzo, E. 2017. The composition of colourless glass: a review. *Archaeological and Anthropological Science*. Vol. 9, pp. 455–483.

Hares, G.B. 1984. Composition and Constitution. In McLellan, G.W., Shand E.B. (Eds.). *Glass Engineering Handbook*, New York, pp. 1.3-1.11.

Henderson, J. 2013. *Ancient glass: an interdisciplinary exploration*, Cambridge University Press.

Hodges H. 1964. *Artifacts. An introduction to early materials and technology*. London.

Hodgkinson, A.K, Frick, D.A. (2020) Identification of cobalt-coloured Egyptian glass objects by la-icp-ms: a case study from the 18th dynasty workshops at Amarna, Egypt. *Mediterranean Archaeology and Archaeometry*, Vol. 20, pp. 45-57.

Huisman, D.J., de Groot, T., Pols, S., Van Os, B.J.H., Degryse P. 2009. Compositional variation in roman colourless glass objects from the Bocholtz burial (the Netherlands). *Archaeometry*. Vol. 51, pp. 413-439.

Humphrey, J.W., Oleson, J.P., Sherwood, A.N. 1998. Greek and Roman technology. *A sourcebook. annotated translations of Greek and Latin texts and document*s. Routledge, London.

Jackson, C. M. 2005. Making colorless glass in the Roman period, *Archaeometry*. Vol. 47, pp. 763–80.

Jackson, C. M., Cottam, S. 2015. A Green Thought in a Green Shade: Compositional and typological observations concerning the production of emerald green glass vessels in the 1st Century A.D. *Journal of Archaeological Science*. Vol. 61, pp. 139–48.

Kaplan, Z., Ipekoglu, B., Boke, Hassan. 2017. Physicochemical properties of glass tesserae in Roman terrace house from ancient *antandros* (base glass, opacifiers and colorants) *Mediterranean Archaeology and Archaeometry*. Vol. 7, pp. 141-157.

Keenan-Jones, D. 2015. Somma-Vesuvian ground movements and the water supply of Pompeii and the Bay of Naples. *American Journal of Archaeology*. Vol. 119, pp. 191–215.

Koleini, F., Philippe Colomban, F., Pikirayi, I., Prinsloo, L.C. 2019. Glass Beads, Markers of Ancient Trade in Sub-Saharan Africa: Methodology, State of the Art and Perspectives. *Heritage.* Vol. 2, pp. 2343–2369.

Liritzis, I, Zakarias, N., Papageorgiou I, Tsaroucha, A., Palamara, E., 2018. Characterization and analyses of museum objects using pXRF: An application from the Delphi Museum, Greece. *Studia Antiqua et Archaeologica*. Vol. 24, pp. 31–50.

Liritzis, I., C. Salter, C, Hatcher, H. 1995. *Chemical composition of some Greco-Roman glass fragments from Patras*, Greece. PACT, Conseil de l'Europe.

Liritzis, I., Laskaris, N., Vafiadou, A., Karapanagiotis, I., Volonakis, P., Papageorgopoulou, C. Bratitsi, M. 2020. Archaeometry: an overview. *Scientific Culture*. Vol. 6, pp. 49-98.

Mirti, P., Davit, P., Gulmini, M. 2002. Colourants and opacifiers in seventh and eight-century glass investigated by spectroscopic techniques. *Analytical and Bioanalytical Chemistry*, Vol. 372, pp. 221–229.

Nenna, M.D, Vichy, M., Picon, M. 1997. L'Atelier de verrier de Lyon, du Ier siècle après J.C., et l'origine des verres Romains. *Revue d'Archèomètrie*. Vol. 2, pp. 81-87.

Neri E., Morvan C., Colomban P., Guerra M.F., Prigent V. 2016. Late Roman and Byzantine mosaic opaque "glass-ceramics" tesserae (5th-9th century). *Ceramics International*. Vol. 42, pp. 18859–18869.

Panagopoulou, A., Lampakis, D., Christophilos, D., Beltsios, K., Ganetsos, Th. (2018) Technological examination of Iznik ceramics BY SEM-EDX, RAMAN, XRD, PLM: a case study. *Scientific Culture*, Vol. 4, pp. 27-33.

Petit- Domínguez, M.D., Giménez, R.G., de Soto, I.S., Rucandio, I. (2014) Chemical and statistical analysis of roman glass from several northwestern Iberian archaeological sites. *Mediterranean Archaeology and Archaeometry*, Vol. 14, pp. 221-235.

Picon, M., Vichy, M. 2003. D'Orient en Occident: l'origine du verre à l'époque romaine et durant le haut Moyen Âge. In: Foy, D., Nenna, M.D. (Eds.). *Échanges et commerce du verre dans le monde antique.* Actes du colloque de l'"Association Francaise pour l'Archéologie du Verre, Aix-en-Provence, Éditions Monique Mergoil, Montagnac, pp. 17-31.

Pouchou, J.L., Pichoir, F. (1991) Quantitative analysis of homogeneous or stratified microvolumes applying the model "PAP", in: K.F.J. Heinrich, D.E. Newbury (Eds.), Electron Probe Quantitation, Springer, US, Boston, MA, pp. 31–75.

Scott, R.B., Degryse, P., 2014. The archaeolgy and archaeometry of natron glass-making. In: Degryse, P. (Ed.), *Glass-making in the Greco-Roman World.* Leuven University Press.

Silvestri, A. 2008. The colored glass of Iulia Felix. *Journal of Archaeological Science*. Vol. 35, pp. 1489-1501.

Silvestri, A., Molin, G., Salviulo, G. 2005. Roman and Medieval glass from the Italian area: bulk characterization and relationships with production Technology. *Archaeometry*. Vol. 47, pp. 797-816.

Silvestri, A., Molin, G., Salviulo, G. 2006. Sand for Roman glass production: an experimental and philological study on source of supply. *Archaeometry.* Vol. 48, pp. 415-432.

Socrates, G. 2001. *Infrared and Raman Characteristic Group Frequencie*s: Table and Charts. Oxford: John Wiley & Sons Ltd.

Torres-Carrasco, M., Palomob., J.G., Puertas, F. 2014. Sodium silicate solutions from dissolution of glass wastes. Statistical analysis. *Materiales de Construcción*. Vol. 64, e014.

Valloto, M., Verità, M. 2002. Glasses from Pompeii and Herculaneum and the sands of the rivers Belus and Volturno. In Renn, J., Castagnetti G. (Eds.). Homo Faber: Studies on Nature. Technology and Science at the Time of Pompeii. Rome, pp. 63–73.

Verità, M. 2004. Natura e tecnologia dei vetri pompeiani attraverso le analisi chimiche dei reperti. In: Beretta M., Di Pasquale G. (Eds). *Vitrum. Il vetro fra arte e scienza nel mondo romano*. Giunti Ed., Prato, pp. 163-167.

Wedepohl, K. H. 1978. *Yttrium and lanthanides, in Handbook of geochemistry*, Vol. II/5, section 39, Springer-Verlag, Berlin, 57–71.

Wedepohl, K. H., Simon, K., Kronz, A. 2011. The chemical composition including the rare earth elements of the three major glass types of Europe and the Orient used in Late Antiquity and the Middle Ages. *Chemie der Erde*. Vol. 71, pp. 289–296.

Wedepohl, K.H., Baumann, A. 2000. The use of marine molluskan shells for Roman glass and local raw glass production in the Eifel area (western Germany). *Naturwissenschaften*. Vol. 87, pp. 129-132.

Zacharias, N., Palamara, E., Kordali, R., Muros, V. (2020) Archaeological glass corrosion studies: composition, environment and content. *Scientific Culture*, Vol. 6, pp. 53-67.